Hindawi Publishing Corporation
Journal of Nanomaterials
Volume 2015, Article ID 826743, 6 pages
http://dx.doi.org/10.1155/2015/826743

Research Article

Size Control of Alloyed Cu-In-Zn-S Nanoflowers

Björn Kempken, Alexandra Erdt, Jürgen Parisi, and Joanna Kolny-Olesiak

Energy and Semiconductor Research Laboratory, Department of Physics, Carl von Ossietzky University of Oldenburg, 26129 Oldenburg, Germany

Correspondence should be addressed to Joanna Kolny-Olesiak; joanna.kolny@uni-oldenburg.de

Received 8 September 2015; Revised 28 October 2015; Accepted 29 October 2015

Academic Editor: Tupei Chen

Uniform, alloyed Cu-In-Zn-S nanoflowers with sizes of 11.5 ± 2.1 nm and 31 ± 5 nm composed of aggregated 4.1 nm and 5.6 nm primary crystallites, respectively, were obtained in a one-pot, heat-up reaction between copper, indium, and zinc acetate with *tert*-dodecanethiol in the presence of trioctylphosphine oxide. Larger aggregates were obtained by diluting *tert*-dodecanethiol with oleylamine, which lowered the reactivity of the indium and zinc precursors and led to the formation of copper rich particles. The thermal decomposition of *tert*-dodecanethiol stabilizing the primary crystallites induced their agglomeration, while the presence of trioctylphosphine oxide on the surface of the nanoflowers provided them with colloidal stability and prevented them from further aggregation.

1. Introduction

"Green" methods of synthesis and environmentally friendly, nontoxic materials gain increasing scientific attention during the last years [1–10]. One of these materials is the Cu-In-Zn-S (CIZS) alloy [3–6, 11–16]. Copper indium disulfide (CIS) and ZnS have similar crystallographic structure and the lattice mismatch between both compounds is relatively small (2.2%); therefore, they can form alloys within the whole composition range [17]. Nanocrystalline CIZS alloys can be synthesized with methods similar to that developed for pure CIS [3]. The synthesis of quasispherical and elongated particles as well as nanocubes of this material has been reported, so far [11, 13, 15, 18–25]. Depending on the composition, CIZS alloys can have bandgaps with values between those of pure ZnS (3.78 eV) and CIS (1.45 eV) [26]. Furthermore, the presence of Zn ions within the CIS lattice can passivate some of the defects, which are usually easily formed in pure CIS, which generally leads to higher emission quantum yields in CIZS alloys, compared to pure CIS [19]. In contrast to pure semiconductor compounds, where the optical properties can be adjusted by the size and the shape of the nanocrystals, due to the quantum size effect [27, 28], the tunability of the bandgap of an alloy is independent from the morphological parameters of the crystallites. This extends the range of possible combinations of optical and electronic properties with sizes and shapes and, thus, the application potential of these nanomaterials. However, for many applications both the properties of isolated nanocrystals in colloidal solution and a possibility to generate larger structures composed of self-assembled nanoparticles are important [29–37]. One of the strategies leading to such larger nanostructures is the limited ligand protection strategy [31], resulting in a controlled aggregation of primary particles and the formation of nanoflower-like geometries. This tactic has been successfully applied to synthesize nanoflowers of several different materials, for example, ZnTe, In_2O_3, $CuInS_2$, or $CuInSe_2$ [30–33, 38, 39].

Here, we describe a one-pot, heat-up synthesis of alloyed CIZS nanocrystals with zinc blende structure, forming uniform, nanoflower shaped aggregates. We attribute the aggregation of the particles to a partial thermal decomposition of the ligand shell. The size of these aggregates could be controlled by changing the composition of the reaction solution, that is, by diluting *tert*-dodecanethiol, which serves as the solvent, one of the ligands and the source of sulfur, with oleylamine.

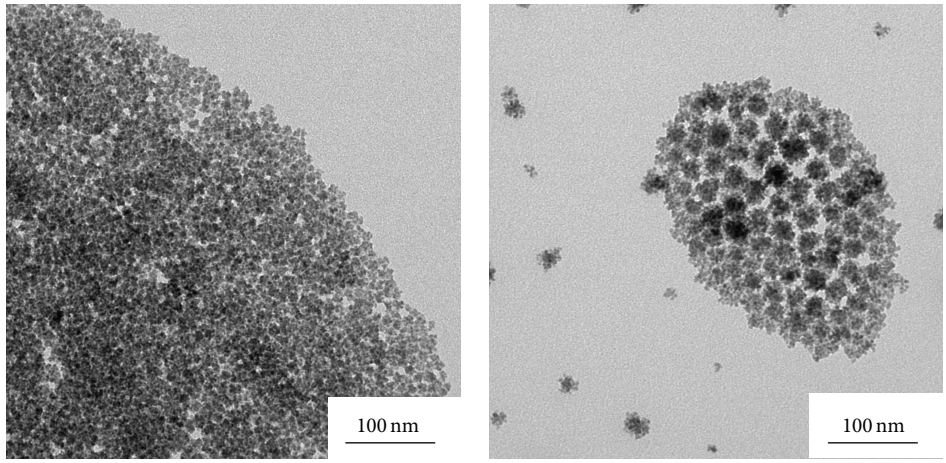

Figure 1: TEM images of CIZS nanoflowers obtained in a reaction in pure t-DDT (a) and in 5 mL t-DDT and 5 mL OLAM (b).

2. Materials and Methods

2.1. Materials. Indium(III)acetate (99.99%—In) ($InAc_3$), copper(I)acetate (99.99%—Cu) (CuAc), zinc(II)acetate (99.99%—Zn) ($ZnAc_2$), oleylamine (OLAM), and *tert*-dodecanethiol (t-DDT) were purchased from Sigma Aldrich. All the chemicals were used without further purification.

2.2. Synthesis. In a typical synthesis 1 mmol copper acetate, 1 mmol indium acetate, 1.7 mmol zinc acetate, and 4.2 mmol TOPO were dissolved in 10 mL t-DDT under vacuum at room temperature. After 10 min the reaction mixture was rapidly heated to 220°C. Aliquots were taken from the reaction solution at different reaction time, between 5 min and 1 h. The resulting nanocrystals were precipitated with ethanol and redissolved in hexane. This cleaning procedure was conducted three times.

2.3. Characterization. Transmission electron microscopy (TEM) images were obtained on a Zeiss EM902A electron microscope with an accelerating voltage of 80 kV. High resolution TEM (HRTEM) micrographs were taken with a JEOL JEM2100F electron microscope. Samples were prepared on a carbon coated copper grid and dried under air for 24 hours. UV/Vis-absorption spectra were taken on a Varian Carry 100 Scan Spectrophotometer and samples were prepared by diluting the solution of the nanocrystal solution with n-hexane. Powder X-ray diffraction (XRD) measurements were performed with a PANalytical X'Pert PRO MPD diffractometer using Cu Kα radiation (1.54 Å), standard Bragg-Brentano θ-2θ geometry, and variable slits. The samples were measured on low background silicon sample holders and prepared by dropping colloidal solution on the holder and letting the solvent evaporate (by heating to 70°C for 30 min). The integral stoichiometry was obtained by the EDAX detector integrated into a FEI Quanta 200 3D scanning electron microscope.

3. Results and Discussion

Alloyed copper indium zinc sulfide nanocrystals were synthesized using a heat-up procedure, starting with copper, indium, and zinc acetate as the sources of the cations. The reaction took place in t-DDT. This ternary thiol can be easily decomposed thermally; therefore, it does not only play the role of the solvent and ligand in this synthesis; but it also serves as the source of sulfur for the growing nanoparticles [11, 18, 40–44]. The thiol is a soft Lewis base, especially capable of stabilizing copper (soft Lewis acid) rich particles, or regulating the activity of the copper monomers in the reaction solution. Because of the presence of In^{3+} ions (hard Lewis acid), TOPO (hard Lewis base) was used as an additional stabilizer.

Particles obtained in this reaction have nanoflower morphology: they are composed of several particles attached together. These aggregates have a uniform size of 11.5±2.1 nm (Figure 1(a)). The size of the nanoflowers increases, when the composition of the reaction solution is changed. Diluting t-DDT with 50% oleylamine results in the formation of larger aggregates of CIZS nanoparticles, with a diameter of 31±5 nm (Figure 1(b)). A closer look at the structure of such aggregates reveals that they are composed of several crystalline domains (Figure 2(a)). Their random orientation is reflected in the random distribution of the spots corresponding to the (111) lattice planes in the fast Fourier transform (FFT) pattern (Figure 2(b)) obtained from the micrograph in Figure 2(a).

The crystallinity of the nanoflowers was further studied by powder X-ray diffraction (see Figure 3). The size of the crystalline domains was calculated from the broadening of the reflections of the XRD pattern using the Debye-Scherrer formula (with $K = 1$ for undefined geometry). The crystallites within the smaller and larger nanoflowers have a diameter of 4.1 nm and 5.6 nm, respectively; thus, the nanoflowers are not single crystalline but consist of several nanoparticles grown together in random orientation, which confirms the observations from HRTEM. These primary particles have

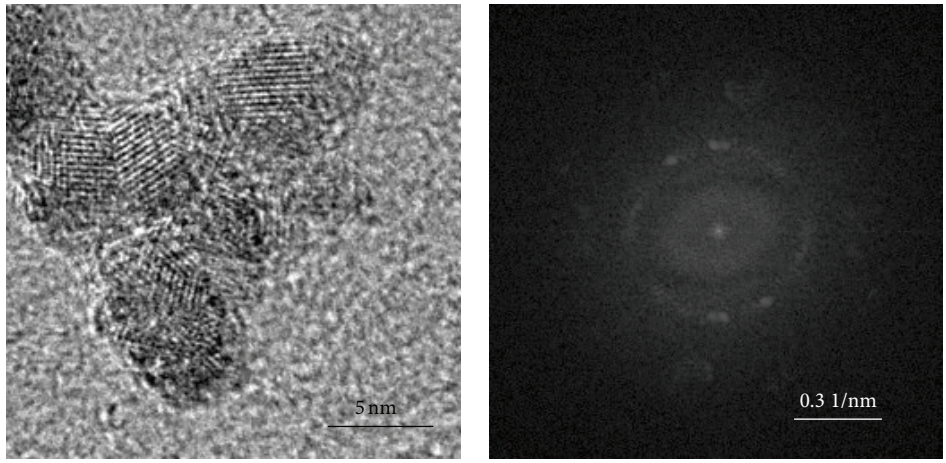

(a) (b)

Figure 2: HRTEM images of CIZS nanoflowers obtained in a reaction in pure t-DDT (a) and the corresponding fast Fourier transform pattern (b).

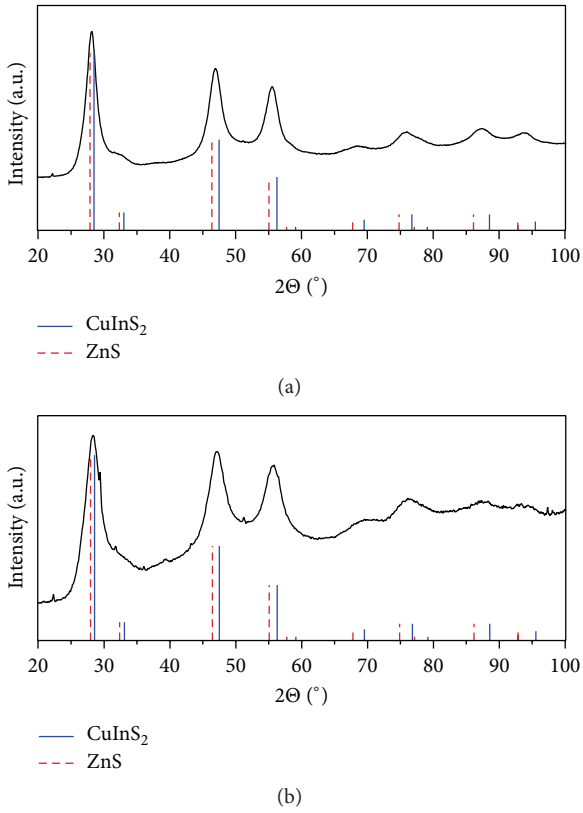

Figure 3: XRD of CIZS nanoflowers obtained in a reaction in pure t-DDT (a) and in 5 mL t-DDT and 5 mL OLAM (b). Reference data is shown for pure ZnS and CIS with zinc blende structure.

zinc blende structure (see Figures 3(a) and 3(b)) and their lattice parameters have values between those for pure CIS and ZnS; this indicates the formation of the CIZS alloy. Assuming a linear dependence between the composition of the alloy and the lattice parameters (Vegard's law), the particles with a lattice constant $a = 5.472$ Å (smaller nanoflowers, Figure 3(a)) and $a = 5.479$ Å (larger nanoflowers, Figure 2(b)) contain 45% and 39% ZnS, respectively.

In order to obtain more precise information about the composition of the particles, the samples were also studied by EDX measurements. The stoichiometry of the smaller nanoflowers is $Cu_{0.71}In_{0.76}Zn_{1.0}S_{2.8}$; thus, the particles are slightly copper deficient (Cu : In ratio is 0.92 : 1) and sulfur rich. Because of the presence of a high concentration of thiols in the reaction solution, we can assume that the particles are, at least partly, stabilized by thiols. Therefore, the excess sulfur atoms are most likely located on the surface of the particles. The ZnS content obtained from EDX is 56%, which is in agreement with the value calculated using Vegard's law.

Not only the size, but also the composition of the nanocrystals is affected by the change of the composition of the solvent. The stoichiometry of the larger nanoflowers is $Cu_{1.31}In_{0.78}Zn_{1.0}S_{3.14}$; thus in contrast to the synthesis without OLAM, the nanocrystals are copper rich. Apparently, the addition of OLAM reduces the activity of indium monomers in the reaction solution, compared with the activity of copper monomers. The In : Zn ratio is not influenced by the composition of the reaction solution; thus, also the reactivity of Zn monomers is affected by the presence of OLAM.

Taking into account the composition of the samples obtained from XRD and EDX, the optical bandgap of the particles should lie in the range between 1.82 and 1.84 eV (values for 39% and 56% ZnS). The bandgap of the particles obtained from the absorption spectrum in Figure 4(a) (smaller nanoflowers) is 2.0 eV [17]. This bandgap widening is most likely a result of the quantum size effect, because the size of the crystallites equals the Bohr radius for CIS (4.0 nm). Another possible reason for the observed larger bandgap value can be the copper deficiency of the particles. A blue shift of the absorption spectra has been observed before for copper poor CIS nanocrystals, which was due to the lowering of

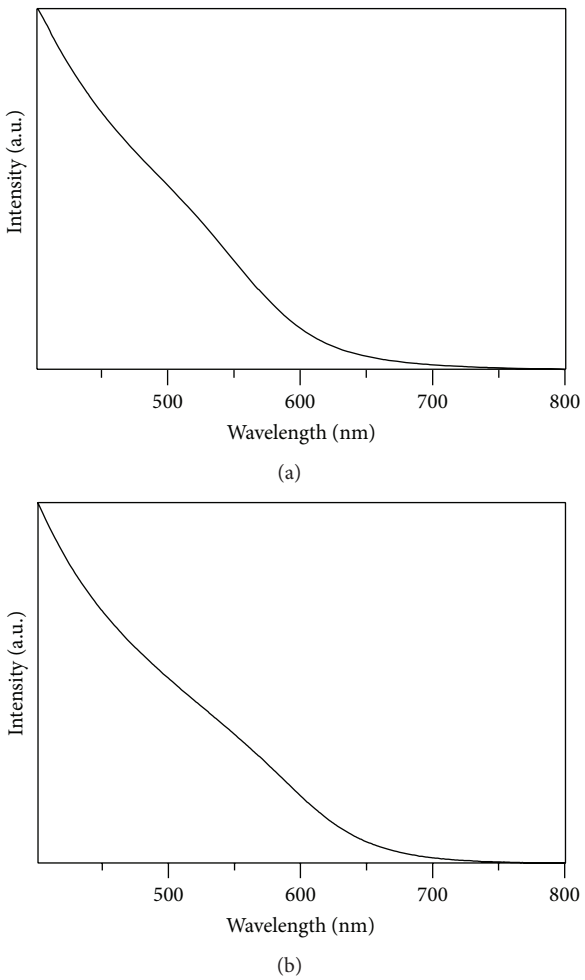

Figure 4: Absorption spectra of CIZS nanoflowers obtained in a reaction in pure t-DDT (a) and in 5 mL t-DDT and 5 mL OLAM (b).

the valence band, determined by the hybridization of the Cu *d* and S *p* orbitals [45]. The absorption spectrum of the larger nanoflowers is slightly red shifted, compared to that of the smaller particles. The reason for the smaller bandgap can be both the larger size and different composition of the particles, especially the higher copper to indium ratio.

The formation of nanoflowers from small nanocrystals indicates changes in the stabilization of the particles during the reaction. In the beginning of the synthesis the surface of the emerging nanocrystals can be passivated in an efficient way, preventing their further growth and, consequently, leading to the formation of relatively small particles (~4–6 nm). The subsequent aggregation of the primary particles is most likely due to the thermal decomposition of t-DDT, which originally passivates the surface copper atoms. Because of the presence of indium ions on the surface of the particles, their ligand shell should also contain TOPO, the other stabilizer molecule. However, in copper rich particles, the fraction of TOPO on the surface should be smaller, and, consequently, the colloidal stability of copper rich primary particles should be lower, compared to particles containing more indium. Therefore, the formation of larger aggregates in the reaction conducted in a mixture of t-DDT and OLAM is most likely due to the larger fraction of t-DDT on the surface of the primary particles. After the thermal decomposition of t-DDT, the colloidal stabilization of the aggregates is due to the presence of thermally stable TOPO molecules; therefore, we expect no further changes in their size during heating of the reaction solution. Indeed, the size of the aggregates remains constant, when they are kept at 220°C for one hour (data not shown here for brevity). Thus, we can conclude that t-DDT is the main ligand stabilizing the primary particles, while the presence of TOPO keeps the nanoflowers in solution and prevents their further aggregation.

4. Conclusions

The use of t-DDT and TOPO as stabilizers is a suitable strategy to synthesize uniform, alloyed CIZS nanoflowers. The low thermal stability of t-DDT is responsible for the aggregation of the primary nanocrystallites, comprising the nanoflowers, while the presence of TOPO provides the agglomerates with sufficient colloidal stability. This strategy, relying mainly on the properties of the organic stabilizing molecules, could be applied to synthesize nanoflowers of other ternary or quaternary copper sulfide based materials, such as copper tin sulfide or copper zinc tin sulfide.

Conflict of Interests

The authors declare that there is no conflict of interests regarding the publication of this paper.

Acknowledgments

The authors gratefully acknowledge funding of the EWE Research Group "Thin Film Photovoltaics" by the EWE AG, Oldenburg. The authors acknowledge also the financial support by the MWN (Material World Network) Program between the National Science Foundation of the US and the Deutsche Forschungsgemeinschaft (Grant no. Li 580/8-1).

References

[1] X. Peng, "Green chemical approaches toward high-quality semiconductor nanocrystals," *Chemistry—A European Journal*, vol. 8, no. 2, pp. 334–339, 2002.

[2] J. A. Dahl, B. L. S. Maddux, and J. E. Hutchison, "Toward greener nanosynthesis," *Chemical Reviews*, vol. 107, no. 6, pp. 2228–2269, 2007.

[3] J. Kolny-Olesiak and H. Weller, "Synthesis and application of colloidal $CuInS_2$ semiconductor nanocrystals," *ACS Applied Materials and Interfaces*, vol. 5, no. 23, pp. 12221–12237, 2013.

[4] Y. Zhao and C. Burda, "Development of plasmonic semiconductor nanomaterials with copper chalcogenides for a future with sustainable energy materials," *Energy and Environmental Science*, vol. 5, no. 2, pp. 5564–5576, 2012.

[5] D. Aldakov, A. Lefrançois, and P. Reiss, "Ternary and quaternary metal chalcogenide nanocrystals: synthesis, properties and

applications," *Journal of Materials Chemistry C*, vol. 1, no. 24, pp. 3756–3776, 2013.

[6] J. Kolny-Olesiak, "Synthesis of copper sulphide-based hybrid nanostructures and their application in shape control of colloidal semiconductor nanocrystals," *CrystEngComm*, vol. 16, no. 40, pp. 9381–9390, 2014.

[7] E. Witt and J. Kolny-Olesiak, "Recent developments in colloidal synthesis of $CuInSe_2$ nanoparticles," *Chemistry—A European Journal*, vol. 19, no. 30, pp. 9746–9753, 2013.

[8] X. Zhang, C. An, S. Wang, Z. Wang, and D. Xia, "Green synthesis of metal sulfide nanocrystals through a general composite-surfactants-aided-solvothermal process," *Journal of Crystal Growth*, vol. 311, no. 14, pp. 3775–3780, 2009.

[9] Z. Zhuang, Q. Peng, and Y. Li, "Controlled synthesis of semiconductor nanostructures in the liquid phase," *Chemical Society Reviews*, vol. 40, no. 11, pp. 5492–5513, 2011.

[10] J.-M. Tarascon and M. Armand, "Issues and challenges facing rechargeable lithium batteries," *Nature*, vol. 414, no. 6861, pp. 359–367, 2001.

[11] J. Li, B. Kempken, V. Dzhagan et al., "Alloyed $CuInS_2$–ZnS nanorods: synthesis, structure and optical properties," *CrystEngComm*, vol. 17, no. 30, pp. 5634–5643, 2015.

[12] R. Xie, M. Rutherford, and X. Peng, "Formation of high-quality I–III–VI semiconductor nanocrystals by tuning relative reactivity of cationic precursors," *Journal of the American Chemical Society*, vol. 131, no. 15, pp. 5691–5697, 2009.

[13] W. Zhang and X. Zhong, "Facile synthesis of ZnS-$CuInS_2$-alloyed nanocrystals for a color-tunable fluorchrome and photocatalyst," *Inorganic Chemistry*, vol. 50, no. 9, pp. 4065–4072, 2011.

[14] D. Deng, Y. Chen, J. Cao et al., "High-quality $CuInS_2$/ZnS quantum dots for in vitro and in vivo bioimaging," *Chemistry of Materials*, vol. 24, no. 15, pp. 3029–3037, 2012.

[15] C. Ye, M. D. Regulacio, S. H. Lim, Q.-H. Xu, and M.-Y. Han, "Alloyed $(ZnS)_x(CuInS_2)_{1-x}$ semiconductor nanorods: synthesis, bandgap tuning and photocatalytic properties," *Chemistry—A European Journal*, vol. 18, no. 36, pp. 11258–11263, 2012.

[16] Q. A. Akkerman, A. Genovese, C. George et al., "From binary Cu_2S to ternary Cu-In-S and quaternary Cu-In-Zn-S nanocrystals with tunable composition via partial cation exchange," *ACS Nano*, vol. 9, no. 1, pp. 521–531, 2015.

[17] D. Pan, D. Weng, X. Wang et al., "Alloyed semiconductor nanocrystals with broad tunable band gaps," *Chemical Communications*, no. 28, pp. 4221–4223, 2009.

[18] M. Kruszynska, H. Borchert, J. Parisi, and J. Kolny-Olesiak, "Synthesis and shape control of $CuInS_2$ nanoparticles," *Journal of the American Chemical Society*, vol. 132, no. 45, pp. 15976–15986, 2010.

[19] J. Zhang, R. Xie, and W. Yang, "A simple route for highly luminescent quaternary Cu-Zn-In-S nanocrystal emitters," *Chemistry of Materials*, vol. 23, no. 14, pp. 3357–3361, 2011.

[20] L. De Trizio, M. Prato, A. Genovese et al., "Strongly fluorescent quaternary Cu-In-Zn-S nanocrystals prepared from $Cu_{1-x}InS_2$ nanocrystals by partial cation exchange," *Chemistry of Materials*, vol. 24, no. 12, pp. 2400–2406, 2012.

[21] X. Tang, W. Cheng, E. S. G. Choo, and J. Xue, "Synthesis of $CuInS_2$-ZnS alloyed nanocubes with high luminescence," *Chemical Communications*, vol. 47, no. 18, pp. 5217–5219, 2011.

[22] J.-Y. Chang and C.-Y. Cheng, "Facile one-pot synthesis of copper sulfide-metal chalcogenide anisotropic heteronanostructures in a noncoordinating solvent," *Chemical Communications*, vol. 47, no. 32, pp. 9089–9091, 2011.

[23] J. Feng, M. Sun, F. Yang, and X. Yang, "A facile approach to synthesize high-quality $Zn_xCu_yInS_{1.5+x+0.5y}$ nanocrystal emitters," *Chemical Communications*, vol. 47, no. 22, pp. 6422–6424, 2011.

[24] G. Manna, S. Jana, R. Bose, and N. Pradhan, "Mn-doped multinary CIZS and AIZS nanocrystals," *Journal of Physical Chemistry Letters*, vol. 3, no. 18, pp. 2528–2534, 2012.

[25] R. Bose, S. Jana, G. Manna, S. Chakraborty, and N. Pradhan, "Rate of cation exchange and change in optical properties during transformation of ternary to doped binary nanocrystals," *Journal of Physical Chemistry C*, vol. 117, no. 30, pp. 15835–15841, 2013.

[26] H. Zhong, Z. Bai, and B. Zou, "Tuning the luminescence properties of colloidal I–III–VI semiconductor nanocrystals for optoelectronics and biotechnology applications," *The Journal of Physical Chemistry Letters*, vol. 3, no. 21, pp. 3167–3175, 2012.

[27] A. P. Alivisatos, "Perspectives on the physical chemistry of semiconductor nanocrystals," *The Journal of Physical Chemistry*, vol. 100, no. 31, pp. 13226–13239, 1996.

[28] M. L. Steigerwald and L. E. Brus, "Semiconductor crystallites: a class of large molecules," *Accounts of Chemical Research*, vol. 23, no. 6, pp. 183–188, 1990.

[29] D. V. Talapin, J.-S. Lee, M. V. Kovalenko, and E. V. Shevchenko, "Prospects of colloidal nanocrystals for electronic and optoelectronic applications," *Chemical Reviews*, vol. 110, no. 1, pp. 389–458, 2010.

[30] Y. Luo, G. Chang, W. Lu, and X. Sun, "Synthesis and characterization of $CuInS_2$ nanoflowers," *Colloid Journal*, vol. 72, no. 2, pp. 282–285, 2010.

[31] A. Narayanaswamy, H. Xu, N. Pradhan, and X. Peng, "Crystalline nanoflowers with different chemical compositions and physical properties grown by limited ligand protection," *Angewandte Chemie International Edition*, vol. 118, no. 32, pp. 5487–5490, 2006.

[32] S. H. Lee, Y. J. Kim, and J. Park, "Shape evolution of ZnTe nanocrystals: nanoflowers, nanodots, and nanorods," *Chemistry of Materials*, vol. 19, no. 19, pp. 4670–4675, 2007.

[33] A. Narayanaswamy, H. Xu, N. Pradhan, M. Kim, and X. Peng, "Formation of nearly monodisperse In_2O_3 nanodots and oriented-attached nanoflowers: hydrolysis and alcoholysis vs pyrolysis," *Journal of the American Chemical Society*, vol. 128, no. 31, pp. 10310–10319, 2006.

[34] Y. Yang, Y. Jin, H. He et al., "Dopant-induced shape evolution of colloidal nanocrystals: the case of zinc oxide," *Journal of the American Chemical Society*, vol. 132, no. 38, pp. 13381–13394, 2010.

[35] J.-Y. Chang, M.-H. Tsai, K.-L. Ou, C.-H. Yang, and J.-C. Fan, "Synthesis of $CuInSe_2$ ternary nanostructures: a combined oriented attachment and ligand protection strategy," *CrystEngComm*, vol. 13, no. 12, pp. 4236–4243, 2011.

[36] Z. Lu and Y. Yin, "Colloidal nanoparticle clusters: functional materials by design," *Chemical Society Reviews*, vol. 41, no. 21, pp. 6874–6887, 2012.

[37] T. Wang, D. LaMontagne, J. Lynch, J. Zhuang, and Y. C. Cao, "Colloidal superparticles from nanoparticle assembly," *Chemical Society Reviews*, vol. 42, no. 7, pp. 2804–2823, 2013.

[38] Z. Sun, Z. Luo, and J. Fang, "Assembling nonspherical 2D binary nanoparticle superlattices by opposite electrical charges: The role of coulomb forces," *ACS Nano*, vol. 4, no. 4, pp. 1821–1828, 2010.

[39] E. Selishcheva, J. Parisi, and J. Kolny-Olesiak, "Copper-assisted shape control in colloidal synthesis of indium oxide nanoparticles," *Journal of Nanoparticle Research*, vol. 14, article 711, 2012.

[40] M. Kruszynska, H. Borchert, J. Parisi, and J. Kolny-Olesiak, "Investigations of solvents and various sulfur sources influence on the shape-controlled synthesis of $CuInS_2$ nanocrystals," *Journal of Nanoparticle Research*, vol. 13, no. 11, pp. 5815–5824, 2011.

[41] J. Li, M. Bloemen, J. Parisi, and J. Kolny-Olesiak, "Role of copper sulfide seeds in the growth process of $CuInS_2$ nanorods and networks," *ACS Applied Materials and Interfaces*, vol. 6, no. 22, pp. 20535–20543, 2014.

[42] A. Singh, J. Ciston, K. Bustillo, D. Nordlund, and D. J. Milliron, "Synergistic role of dopants on the morphology of alloyed copper chalcogenide nanocrystals," *Journal of the American Chemical Society*, vol. 137, pp. 6464–6467, 2015.

[43] X. Zhang, N. Bao, K. Ramasamy et al., "Crystal phase-controlled synthesis of Cu_2FeSnS_4 nanocrystals with a band gap of around 1.5 eV," *Chemical Communications*, vol. 48, no. 41, pp. 4956–4958, 2012.

[44] C.-M. Fan, M. D. Regulacio, C. Ye et al., "Colloidal nanocrystals of orthorhombic Cu_2ZnGeS_4: phase-controlled synthesis, formation mechanism and photocatalytic behavior," *Nanoscale*, vol. 7, no. 7, pp. 3247–3253, 2015.

[45] M. Uehara, K. Watanabe, Y. Tajiri, H. Nakamura, and H. Maeda, "Synthesis of $CuInS_2$ fluorescent nanocrystals and enhancement of fluorescence by controlling crystal defect," *The Journal of Chemical Physics*, vol. 129, no. 13, Article ID 134709, 6 pages, 2008.